

**A Global Model for Predicting the Burning Rates
of Liquid Pool Fires**

Anthony Hamins, Jiann C. Yang, and Takashi Kashiwagi

Building and Fire Research Laboratory
Gaithersburg, Maryland 20899



United States Department of Commerce
Technology Administration
National Institute of Standards and Technology

A Global Model for Predicting the Burning Rates of Liquid Pool Fires

Anthony Hamins, Jiann C. Yang, and Takashi Kashiwagi

September 1999
Building and Fire Research Laboratory
National Institute of Standards and Technology
Gaithersburg, MD 20899



U.S. Department of Commerce
William M. Daley, *Secretary*
Technology Administration
Gary R. Bachula, *Acting Under Secretary for Technology*
National Institute of Standards and Technology
Raymond G. Kammer, *Director*

CONTENTS

ACKNOWLEDGMENTS	iv
ABSTRACT.....	v
INTRODUCTION	1
MODEL FORMULATION	2
Radiation.....	5
Convection	6
Conduction.....	7
RESULTS AND DISCUSSION	8
CONCLUSIONS.....	11
REFERENCES	23

ACKNOWLEDGMENTS

The authors are grateful to Professor J. Gore, Dr. M. Klassen, Professor J. Quintiere for many helpful discussions, and to David Mattingly for performing some of the calculations. The authors would also like to thank Ken Steckler and Dr. Steven J. Ritchie for their useful comments in improving the first draft of this report.

ABSTRACT

A global model is presented which predicts the mass burning flux for pool fires consuming liquid fuels in a quiescent environment. The model assumes constant bulk properties such as flame temperature, soot volume fraction, and species concentration. The computational procedure requires knowledge of the fuel smoke point height and fuel properties such as the heat of vaporization, heat capacity, and boiling point. A cylindrical flame shape is assumed with the flame height given by Heskestad's correlation. A mean beam length approach for radiative heat transfer is utilized and emission from both gas species and soot particles is considered. The convective heat transfer coefficient is estimated using a Raleigh number correlation. Experiments in small diameter pool fire are used to quantify the conductive heat transfer. The predicted mass flux for a number of fuels is within a factor of two of measured burning rates for pool diameters greater than 0.2 m.

INTRODUCTION

The mass flux of burning fuel in a pool fire depends on the heat feedback from the flame to the fuel surface, which occurs in the form of conductive, convective, and radiative heat transfer. The relative contribution of each of these components depend on a large number of parameters including pool diameter, burner material, lip height, flame shape, and the spatial distribution of temperature, species concentration and soot volume fraction. The goal of the present study is to develop a predictive algorithm for burning flux which is consistent with the essential physics of the problem and which is also generic, such that experimental determination of parameters in the model is not required for each new fuel or pool diameter considered.

A number of burning rate models have been developed using a global approach. [1,2,3,4,5,6] The heat feedback, \dot{Q} (W), to the pool surface is the sum of conduction (\dot{Q}_{cond}), convection (\dot{Q}_{conv}), and radiation (\dot{Q}_{rad}):

$$\dot{Q} = \dot{Q}_{cond} + \dot{Q}_{conv} + \dot{Q}_{rad} \quad (1)$$

The model considers the fuel to be isothermal horizontally and to be steadily burning. Hottel [1] represented heat transfer to the pool surface in terms of characteristic or global flame properties:

$$\dot{Q}_{cond} = k \pi D (T_f - T_s) \quad (2)$$

$$\dot{Q}_{conv} = h A_s (T_f - T_s) \quad (3)$$

$$\dot{Q}_{rad} = \sigma F A_s (T_f^4 - T_s^4) (1 - e^{-\Gamma D}) \quad (4)$$

where k (W/m-K) is a conduction coefficient, D (m) is the pool diameter, A_s (m^2) is the pool surface area, T_f (K) is the flame temperature, T_s (K) is the pool surface temperature, h (W/m² K) is a convective heat transfer coefficient, σ is the Stefan-Boltzmann constant (5.67×10^{-8} W/m² K), F is a dimensionless flame-pool surface radiative view factor, and Γ (m^{-1}) is a radiative extinction coefficient.

Hottel noted that when D is small, conduction dominates because convection and radiation are proportional to D^2 . When D is large conduction becomes unimportant and radiation eventually dominates convection, because ΓD becomes large and radiation is proportional to T_f^4 .

Global burning rate models have been discussed by a number of other researchers. Hayasaka and Koseki [2] used a mean beam length model with global flame properties and compared their predictions with measured burning rates for pools up to 10 m in diameter. Their model, however, has not been tested on fuels other than kerosene. Modak and Croce [3] calculated the radiative heat flux from the flame to a surface element on a burning pool (0.18 m) of PMMA in terms of an empirical time-averaged flame shape, an effective radiation temperature, and a mean

gray-body absorption-emission coefficient. These parameters were all independently measured whereas convection was assumed to be negligible. Orloff and de Ris [4,5] represented the fire as a time averaged volume of constant property gases. Their measured radiative heat loss fraction (χ_R) was used to estimate a global absorption-emission coefficient. Measured flame shapes were used to calculate a mean beam length. Convective heat feedback was estimated from experiments on a water cooled gas burner. Model predictions were compared to measurements for several experimental conditions for pools burning liquid methanol and solid thermoplastics. An attempt to validate their model for liquid fuels other than methanol was not successful. This may be because flame shapes can vary dramatically for different fuels (as a function of stoichiometry) and thus time averaged shapes must be determined for each fuel of interest.

MODEL FORMULATION

We consider the mass burning rate of a liquid fuel in a metal burner of internal diameter D . The case of small lip height (l) and moderate pool depth (d) is examined (see Fig. 1). Heat flux (W/m^2) feedback to the pool surface is based on Eq. 1. The burning rate is taken as the sum of conduction (\dot{Q}_{cond}), convection (\dot{Q}_{conv}), radiation (\dot{Q}_{rad}), and re-radiation (\dot{Q}_{rerad}) from the pool surface:

$$\dot{M}[H_v + C_{pf}(T_s - T_a)] = \dot{Q}_{cond} + \dot{Q}_{conv} + \dot{Q}_{rad} - \dot{Q}_{rerad} \quad (5)$$

The heat feedback represents the energy required to vaporize the liquid fuel where \dot{M} (g/s) is the mass burning rate, H_v (J/g) is the heat of vaporization at T_s (K), C_{pf} (J/g K) is the liquid heat capacity, and T_a (K) is the bulk fluid temperature at ambient condition. Equation 5 assumes that all heat to the pool surface goes to vaporize the fuel, *i.e.*, heat losses for these deep pools ($d > 10$ cm) and increases in the sensible heat of the liquid fuel are negligible. In our model, \dot{Q}_{cond} represents heat transfer from the fire through the burner walls into the liquid pool.

The flame is modeled as a homogeneous mixture of entrained air, combustion products (CO_2 , H_2O , and soot), unburnt fuel, and inert N_2 at a global flame temperature. The global temperature, T_f , is calculated from an enthalpy balance about a control volume encompassing the gas-phase cylindrical flame. The amount of entrained air entering the flame is determined from Reference [7], modified by a constant factor which is determined from a best fit of the burning rate data. This form of the global temperature was chosen only after trying a number of approaches to find a suitable representative global temperature, including a constant temperature (1000 K, 1100 K, 1200 K, *etc.*) and a temperature based on the average of the calculated maximum flame temperature and the surface temperature (T_s), which was assumed to be at the boiling point. These forms led to poor predictions of the burning rate.

T_f is calculated in a manner similar to Smith and Van Ness [8]. The effects of radiative heat losses, combustion efficiency, and dilution by air entrainment are also considered. The energy available to heat the excess entrained air, combustion products, and unburnt fuel to T_f is equal to the heat of combustion, H_c (J/mol), less the energy due to losses associated with radiative loss

(χ_R), combustion efficiency (χ_a), and the heat of vaporization of the fuel, H_v (J/mol), at ambient temperature, T_a (K):

$$(\chi_a - \chi_R) H_c - H_v = \sum_i \int_{T_a}^{T_f} X_i C_{p,i}(T) dT \quad (6)$$

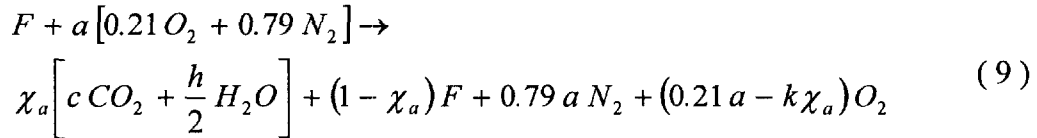
where $C_{p,i}(T)$ (J/mol K) is the vapor heat capacity [9] of the i^{th} gaseous species, which includes N_2 , CO_2 , H_2O , unburnt fuel, and excess O_2 , and X_i is the mole fraction of the i^{th} gaseous species. The radiative heat loss fraction is defined as:

$$\chi_R = \frac{\dot{Q}_r}{\dot{M} H_c / MW} \quad (7)$$

where \dot{Q}_r (W) is the energy emitted by the flame to the surroundings. The combustion efficiency is defined as:

$$\chi_a = \frac{H_a}{\dot{M} H_c / MW} \quad (8)$$

where H_a (W) is the actual heat release rate and $\dot{M} \cdot H_c / MW$ (W) represents the ideal heat release, where MW is the fuel molecular weight (g/mol). The concentrations (X_i) of CO_2 , H_2O , N_2 and O_2 are determined from stoichiometry and the amount of entrained air. The concentration of unburnt fuel is determined from the combustion efficiency. The chemical reaction for 1 mole of fuel (F) containing " c " carbon atoms, " h " hydrogen atoms, and " o " oxygen atoms mixing with entrained air in the flame is represented as:



where k is a constant = $[c + (h/4) - (o/2)]$ and a is the moles of air (= $M_a / [28.96 \text{ g/mol}]$) entrained into the fire. The mass of air per unit time (M_a) entrained into a fire of height H , is given by [7] (in units of kg/s):

$$M_a = 0.086(H')^{0.5} (r \chi_a + 1) D^2 Fr c' \quad \text{for } H' < 1 \quad (10)$$

$$M_a = 0.093(H')^{1.5} (r \chi_a + 1) D^2 Fr c' \quad \text{for } 1 < H' < 4 \quad (11)$$

$$M_a = 0.018(H')^{2.5} (r \chi_a + 1) D^2 Fr c' \quad \text{for } H' > 4 \quad (12)$$

where H' ($= H/D$) is a non-dimensional flame height and c' is an empirically determined dimensionless parameter ($= 0.11$), universal for all fuels, and r is the stoichiometric mass ratio of fuel to air. The Froude number is defined as:

$$Fr = \frac{Q_D^* R'}{H_c \sqrt{\frac{H_c (\chi_a - \chi_R)}{R'}}} \quad (13)$$

where $R' = (r \chi_a + 1) C_{pa} T_a$ and $Q_D^* = \frac{\dot{M} H_c}{\rho_a C_{pa} T_a D^2 \sqrt{g D}}$

Intermediate gas species (CO, H₂, etc.) and soot are neglected in the temperature calculation, except in a global sense through χ_a . Table 1 summarizes some of the fuel parameters used in the temperature calculation including the fuel type, the radiative heat loss fraction (χ_R) [6,10,11], the combustion efficiency (χ_a) [10] and the characteristic soot volume fraction (f_v) which is discussed below. The calculated flame temperature (T_f) is a weak function of diameter as the fuel/air entrainment varied. T_f for a 1 m diameter pool is given in Table 1.

Table 1 Summary of fuel parameters used in the model including fuel type, radiative heat loss fraction (χ_R), combustion efficiency (χ_a), soot volume fraction (f_v), and the calculated global flame temperature (T_f) for a 1 m diameter pool fire.

Fuel	χ_R	χ_a	$f_v \times 10^{-6}$	T_f (K)
Methanol	0.20 ^b	1.0 ^a	0.0	1114
Ethanol	0.23 ^a	0.92 ^a	0.07	1034
Acetone	0.26 ^a	0.94 ^a	0.11	1042
MMA	0.34 ^b	0.88 ^a	0.22	933
Hexane	0.30 ^a	0.93 ^a	0.29	1007
Heptane	0.30 ^b	0.92 ^a	0.50	1010
Toluene	0.32 ^b	0.76 ^d	6.0	843
Benzene	0.35 ^c	0.76 ^c	6.8	802

^aReference [10]

^bReference [11]

^cReference [6]

^dmeasured in cone calorimeter [12]

^eassumed equal to χ_a for toluene

Radiation

Heat transfer to the surface of the pool by radiation is modeled as isothermal emission from gaseous CO₂ and H₂O and gray-body emission from soot. A correction for spectral overlap by these emitters was included. Total radiation to the pool surface (\dot{Q}_{rad}) was given by Siegel and Howell [13]:

$$\dot{Q}_{rad} = \sigma T_f^4 A_s (1 - \rho) [1 - (1 - \varepsilon_{soot})(1 - \varepsilon_w)(1 - \varepsilon_c)] \quad (14)$$

where ρ (= 0.08) is the surface reflectivity for liquid fuels [14], ε_{soot} is the spectrally averaged emissivity of soot, ε_w is the total emissivity of H₂O, and ε_c is the total emissivity of CO₂. Gas emission and absorption by fuel vapor, CO and other gas species is not considered here. Gas emissivity for CO₂ and H₂O are calculated using the algorithm given by Leckner [15]. Reflection of the incoming radiation is dependent on the angle of incidence. A value of 0.08 is a reasonable value for pool fires, regardless of fuel type [14].

Yuen and Tien [16] have shown that soot emission can be approximated by the following expression for a gray emitter:

$$\varepsilon_{soot} = 1 - e^{-\kappa L} \quad (15)$$

In the above equation, L is the path length and κ is the effective soot emission parameter:

$$\kappa = \frac{3.6 C_1 T_f}{C_2} \quad (16)$$

where C_2 is Plank's second constant (0.014388 m K) and the dimensionless effective soot concentration parameter, C_1 , is defined as:

$$C_1 = \frac{36 \pi f_v n^2 s}{[n^2 - (ns)^2 + 2]^2 + 4n^4 s^2} \quad (17)$$

The infrared averaged optical constants ($n = 3.49$ and $s = 2.17$) for soot particles were taken from Tien and Lee [17]. For a particular flame geometry, the assumption of a homogeneous gray mixture allows use of the mean beam length (L_m) to represent the characteristic path length, L , (see Eq. 15). For simplicity, the flame is assumed to be a right cylinder, and the mean beam length is given by [5]:

$$L_m = \frac{3.6V}{A_f} \quad (18)$$

where V is the flame volume and A_f is the flame surface area. For a right cylinder, the flame volume and surface area are given by:

$$V = \pi R^2 H \quad (19)$$

$$A_f = 2\pi R(R + H) \quad (20)$$

where R is the pool radius and H is the flame height determined using the correlation given by Heskestad [18].

A number of studies have measured soot volume fraction distributions in pool flames burning liquid fuels [11,19] whereas only a few studies have systematically studied the effects of scale or fuel type. Bard and Pagni [20] measured the soot volume fraction 0.03 m above the surface of 0.20 m diameter pool fires for a number of fuels. Whereas f_v changes as a function of location in the flame, Bard and Pagni's measurements were taken as representative of the soot volume fraction. For fuels that Pagni did not measure, a correlation with smoke point height (l_s) is used. The smoke point height characterizes the sooting propensity of fuels and has been measured for an extensive number of fuels [10,21,22]. Figure 2 shows Pagni's f_v measurements as a function of fuel smoke point height. Although it is possible that combustion characteristics may vary as a function of pool diameter, not enough reliable measurements exist to determine that dependence. The existing data suggest that for pool diameters less than 2 m, χ_a and χ_R are independent of scale [23]. Because of the relationship between f_v and χ_a , as shown in Fig. 2, the model also assumes that f_v is a function of fuel type only. Variation of combustion characteristics as a function of pool diameter can be easily incorporated into the present model.

Because of the relatively low boiling point of these fuels, re-radiation from the pool surface to the ambient [4,5]:

$$\dot{Q}_{rerad} = \sigma A_s (T_s^4 - T_a^4) \quad (21)$$

is very small compared to convection or radiation.

Convection

Convective heat transfer to the fuel surface is approximated using the stagnant film model [4,5]:

$$\dot{Q}_{conv} = A_s \frac{h'}{C_{pa}} \left[\frac{H_c (\chi_a - \chi_R) r}{\chi_a} - C_{pa} (T_s - T_a) \right] \frac{y}{e^y - 1} \quad (22)$$

where $y = \dot{M} (C_{pa} / h') / A_s$ is a blowing factor which effectively reduces heat transfer as mass transfer increases. The symbol r represents the stoichiometric air/fuel mass ratio and C_{pa} is the effective heat capacity of air taken at a representative temperature equal to $(T_f + T_s)/2$. A simple

heat transfer coefficient (h') is used, based on a Rayleigh number criterion for natural convective heat transfer on a hot surface facing upwards [24]:

$$\begin{aligned} h' &= 0.54 Ra^{0.25} & 10^5 < Ra < 2 \cdot 10^7 \\ h' &= 0.14 Ra^{0.33} & 2 \cdot 10^7 < Ra < 3 \cdot 10^{10} \end{aligned} \quad (23)$$

h' takes on values typically ≈ 9 W/m² K, which is consistent with the value used by Orloff and de Ris ($h' \approx 7$ W/m² K) for pools with finite height lips [4,5]. If convective transfer to the pool surface is modeled as flow past a cavity, then the effect of lip height on h' is small [25], and use of the same value of h' to model convective transfer in a fire without a finite lip height is not unreasonable.

Conduction

Conduction from the flame to the fuel surface is modeled as one-dimensional heat transfer vertically down through the burner walls. All heat is assumed to be transferred into the liquid pool:

$$\dot{Q}_{cond} = k_b A_w \frac{dT}{dz} \quad (24)$$

where k_b (W/m K) is the thermal conductivity of the burner and is material dependent, dT/dz (K/m) is the thermal gradient in the wall and A_w (m²) is the wall cross sectional area:

$$A_w = \frac{\pi(D_o^2 - D^2)}{4} \quad (25)$$

where D_o (m) is the outer diameter and D (m) the inner diameter of the pan.

To determine the thermal gradient dT/dz in Eq. 24, temperature measurements were made inside the walls of brass burners. The experimental set-up has been described previously [11]. Thermocouples were spaced 0.003 m apart (0.001 m, 0.004 m, and 0.007 m below the burner rim) and in the center of the brass wall of a 0.035 m diameter pool. During each burn a constant lip height (0.007 m) was maintained. A temperature gradient of 160 K/m was measured a few seconds after ignition which remained constant during the entire experiment (20 min). Decreasing the lip height to 0.005 m did not change the temperature gradient. Nor did the temperature gradient change for a 0.050 m diameter pool with 0.005 m lip height and 0.0032 m brass walls. Thermocouples mounted 0.001 m and 0.002 m into the walls 0.001 m below the burner rim measured the same temperatures (within 0.1 K) as a function of time from flame ignition, indicating that the assumption of one-dimensional vertical heat conduction is appropriate. Table 2 lists the conditions and results for ethanol burning rate experiments. The total conductive heat transfer down through the burner walls increased for the larger pool, but the conductive flux normalized by the pool surface area increased only slightly.

Using Eq. 24, the total energy conducted (\dot{Q}_{cond}) to the fuel increases with pool diameter (D) as noted in Table 2, whereas the energy conducted per unit wall area (\dot{Q}_c'') is approximately constant.

Table 2 Pool diameter (D), burner wall thickness, measured thermal gradient inside of the burner walls, total conductive heat transfer through the burner walls (\dot{Q}_{cond}), and average conductive heat transfer per unit area of pool surface (\dot{Q}_c'') for pools with brass walls burning ethanol.

D (m)	Wall (m)	dT/dz (K/m)	\dot{Q}_{cond} (W)	\dot{Q}_c'' (W/m ²)
0.035	0.0020	$160 \pm 10^*$	3.9	4100 ± 400
0.050	0.0032	160 ± 10	8.8	4500 ± 500
*the uncertainty is expressed as 1σ .				

RESULTS AND DISCUSSION

The required input for the model are physical parameters such as the fuel heat of vaporization, liquid and vapor fuel heat capacity, the fuel boiling temperature, the burner material composition and wall thickness, and the combustion characteristics of the fuel such as the stoichiometry, combustion efficiency, the radiative heat loss fraction and the soot volume fraction. The model was tested on a variety of liquid fuels over a range of pool diameters from 0.1 m to 2.5 m. The fuels tested include methanol, ethanol, acetone, methyl methacrylate (MMA), hexane, heptane, benzene and toluene. These fuels yield flames with a wide range of flame luminosities, heat release rates, and soot volume fractions.

The predicted mass burning flux was calculated by solving Eq. 5 iteratively. The range of pool diameters considered was from 0.1 to 2.5 m. The upper bound was limited by measurements available in the literature. Conduction was modeled by assuming that the burner material was brass with walls 0.002 m thick. These conditions were chosen as representative in order to quantitatively model conduction, and realizing that the conditions vary widely from experiment to experiment. The calculations showed that conduction is small compared to convection and radiation.

Table 3 lists values of the ratio of the mean beam length to pool diameter, the ratio of flame height to pool diameter, and the emissivities of soot, CO₂ and H₂O as a function of fuel type and pool diameter. For each fuel, the ratio of mean beam length to pool diameter is nearly independent of diameter indicating that the absolute value of the mean beam length is proportional to pool diameter. The ratio of flame height to diameter decreases weakly as a function of pool diameter. The flame heights and the mean beam lengths for methanol are much smaller than heptane or toluene. The values of the emissivities are functions of stoichiometry, temperature and mean beam length and thus vary with fuel and pool diameter. As expected, the soot emissivity for toluene is

the highest whereas the gaseous emissivities for the three fuels are comparable. The magnitude of the values are in line with those determined previously [26].

Figures 3-10 compare measured mass burning fluxes to those predicted by the model as a function of pool diameter for the fuels listed in Table 1. The experimental measurements were compiled from a large number of studies [11,14,19,,27,28,29,30,31,32]. The scatter in the experimental data, as in Fig. 8 for example, may be attributed to differences in the experimental method, burner material, environmental conditions (quiescent or windy), lip height, use of water cooling, etc. Whereas a few experiments have been performed under quasi "steady state" conditions with a constant lip height accomplished by replenishing the fuel (filled symbols in Figs. 3-10), most experiments have been conducted under free burn conditions where the lip height increases with time (open symbols in Figs. 3-10). As the lip height increases, large changes in the radiative heat transfer can occur as the view angle from flame to fuel surface decreases. The convective heat transfer may also decrease. Because the number of constant lip height burning flux measurements in the literature are limited, additional measurements were made using the apparatus and methods described previously [11]. In Figs. 3-10, both constant and varying lip height data are plotted. Steady lip height burning rate data are indicated by the filled symbols and burn-down (varying lip height) data are denoted by the hollow symbols. Only a few measurements are available to compare burning fluxes under conditions of constant versus varying lip height (for the same diameter pool). Fig. 3 ($D = 0.3$ m and 0.6 m), Fig. 4 ($D \approx 0.3$ m), Fig. 8 ($D = 0.6$ m) and Fig. 10 ($D = 0.6$ m) show the same burning flux regardless of lip height conditions whereas only Fig. 8 ($D = 0.3$ m) shows some difference in burning fluxes. For these reasons, all available measurements are compared to the calculations presented here.

Figures 3-10 show that the burning rate model calculations agree with experiment to within approximately a factor of 2 for pool diameters greater than 0.2 m. The largest differences occur for small pool diameters (< 0.2 m) where the model was within a factor of three or better.

The sensitivity of the burning flux calculation to variation of input parameters was assessed by defining a sensitivity coefficient (S_i) such that:

$$S_i = \frac{\Delta m / m}{\Delta p_i / p_i} \quad (26)$$

where $(\Delta m/m)$ was the percentage change in the mass burning flux and $(\Delta p_i/p_i)$ was the percentage change in one of the input parameters χ_a , χ_R , f_v , or T_f . The sensitivity coefficients determined for the 0.30 m heptane and methanol pools are presented in Table 4. S_i varies only slightly with pool diameter for each of these fuels. A negative sensitivity coefficient indicates a decrease in mass burning flux for an increase in the perturbed parameter. Table 4 shows that the largest change in burning rate occurs for a perturbation of temperature, followed by χ_a , χ_R , and f_v . If the global temperature estimate is good to 150 K, then the burning flux calculation is accurate to 50 % for heptane and 40 % for methanol.

Figure 11 compares the calculated and measured [14] percentage of radiative transfer as a function of pool diameter for methanol, heptane and toluene fires. For all fuels, the relative

contribution of radiation increases with pool diameter. As expected from the χ_R data, radiative heat transfer to the pool surface is most important for toluene followed by heptane and methanol respectively, for all pool diameters.

Table 3 The calculated values of the ratio of the mean beam length (L_m) to pool diameter (D), the ratio of flame height (H) to pool diameter (D), and the emissivities of soot (ϵ_{soot}), H_2O (ϵ_w) and CO_2 (ϵ_c).

Fuel	D (m)	L_m/D	H/D	ϵ_{soot}	ϵ_w	ϵ_c
Methanol	0.05	0.72	2.0	0	0.028	0.037
	0.1	0.70	1.8	0	0.046	0.049
	0.5	0.68	1.5	0	0.13	0.081
	1	0.66	1.4	0	0.18	0.097
Heptane	0.05	0.82	4.8	0.014	0.023	0.042
	0.1	0.81	4.3	0.028	0.039	0.055
	0.5	0.80	4.2	0.13	0.11	0.088
	1	0.80	4.1	0.25	0.16	0.10
Toluene	0.05	0.80	4.2	0.13	0.020	0.047
	0.1	0.80	4.1	0.24	0.034	0.060
	0.5	0.80	4.0	0.75	0.095	0.093
	1	0.79	3.7	0.94	0.14	0.11

Table 4 Sensitivity of the Model to Input Parameters for 0.3 m diameter pool fires.

Parameter	S_i	
	Heptane	Methanol
χ_R	-0.90	-0.5
χ_a	2.1	1.8
f_v	0.2	*
T_f	3.5	2.9

* S_i not defined because $f_v = 0$ for methanol pool fires.

CONCLUSIONS

A simple global model for predicting the burning rates of liquid fuels has been developed. The model requires the input of fuel properties (C_{pf} , H_v , boiling temperature, *etc.*) and fuel combustion characteristics (χ_a , χ_R , and f_v). Smoke point height measurements for an extensive number of fuels are available in the literature as are correlations of χ_a , χ_R , and f_v with l_s [10,21,23]. For other fuels, a single simple experiment would be necessary to obtain l_s [33]. Thus, the model described here requires no input other than physical properties of the fuel and the fuel smoke point height.

Although a comparison of the results of the model with measurements are encouraging, further work is required to systematically measure the mass burning flux for large (> 0.60 m) diameter pools under conditions of steady lip heights where few or no data currently exist. In addition, the importance of radiative absorption by fuel vapor is under study by use of absorption spectroscopy.

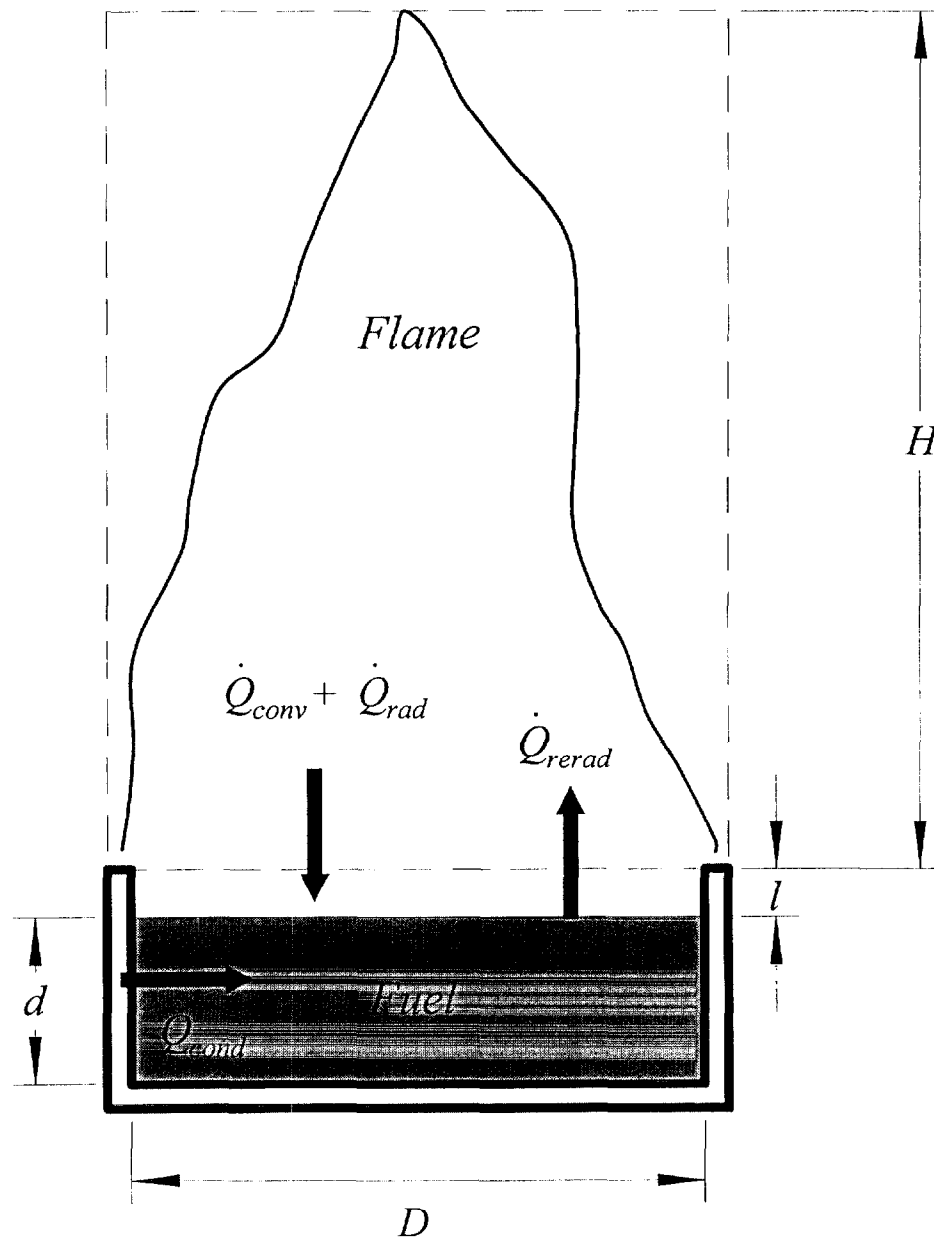


Figure 1. Schematics showing various heat transfer mechanisms associated with a liquid pool fire.

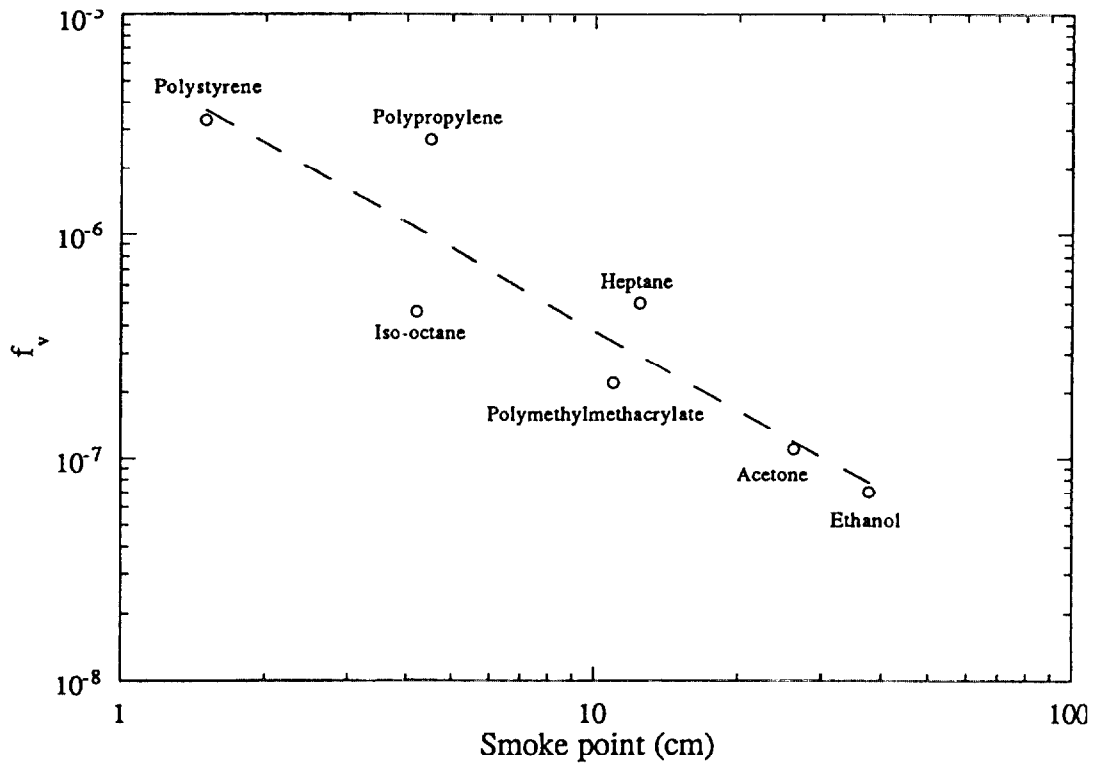


Figure 2. Characteristic value of the soot volume fraction in a pool fire [20] as a function of the smoke point height [10] for a number of different fuels.

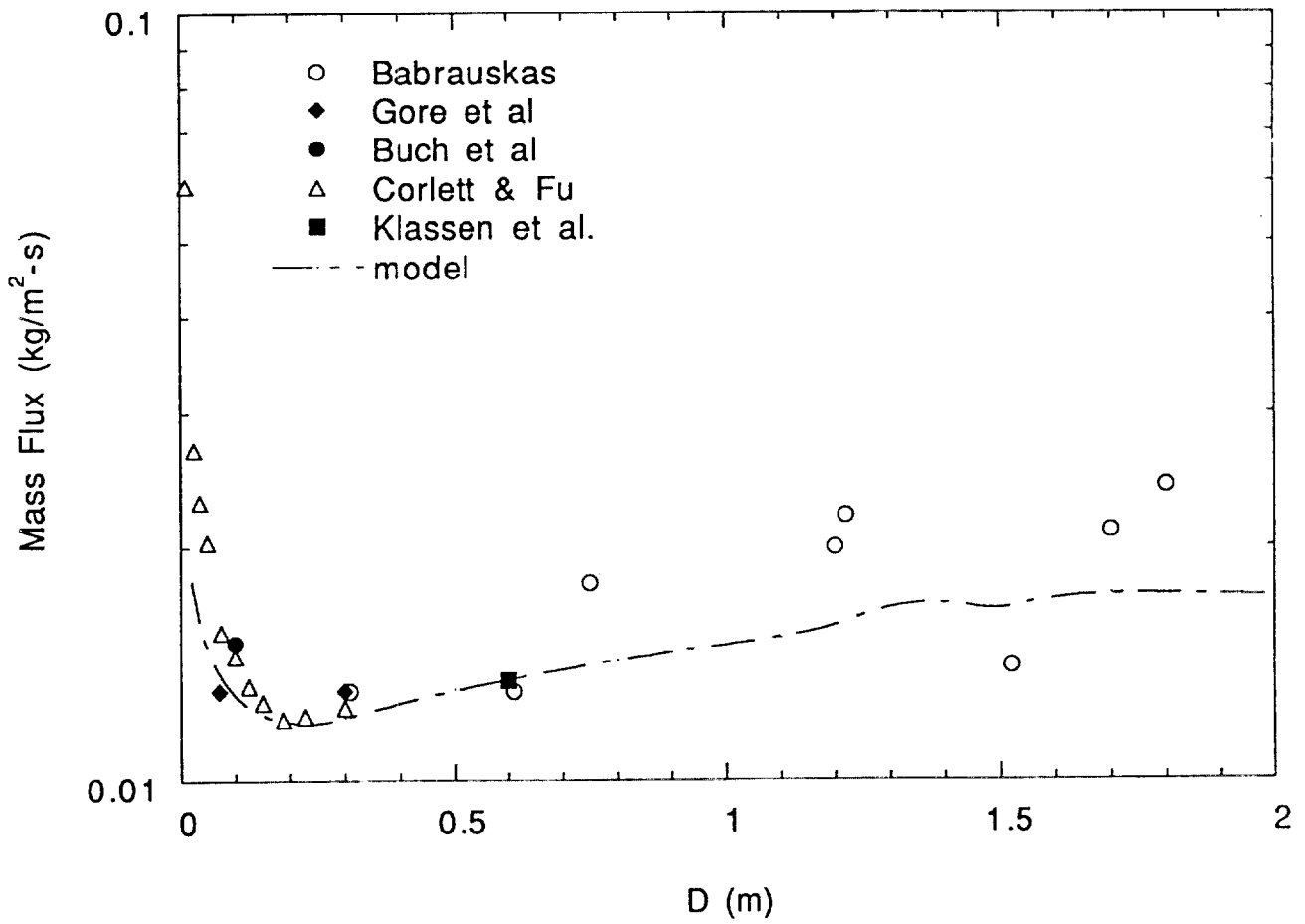


Figure 3. Comparison of experimentally measured mass burning fluxes to those predicted by the model for methanol as a function of pool diameter. Filled symbols represent measurements where the lip height was maintained at a constant value. Open symbols represent measurements where the lip height was varying.

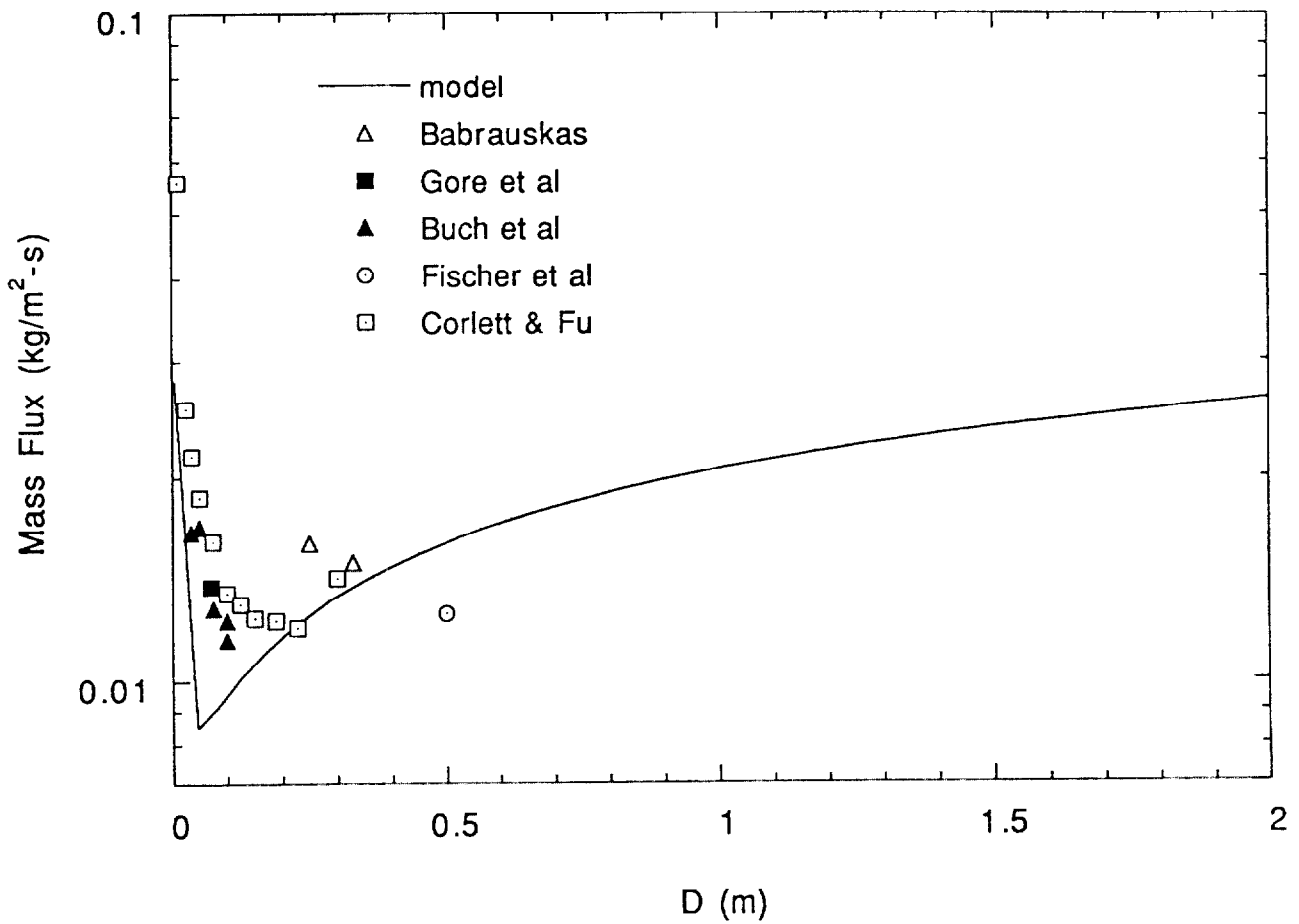


Figure 4. Comparison of experimentally measured mass burning fluxes to those predicted by the model for ethanol as a function of pool diameter. Filled symbols represent measurements where the lip height was maintained at a constant value. Open symbols represent measurements where the lip height was varying.

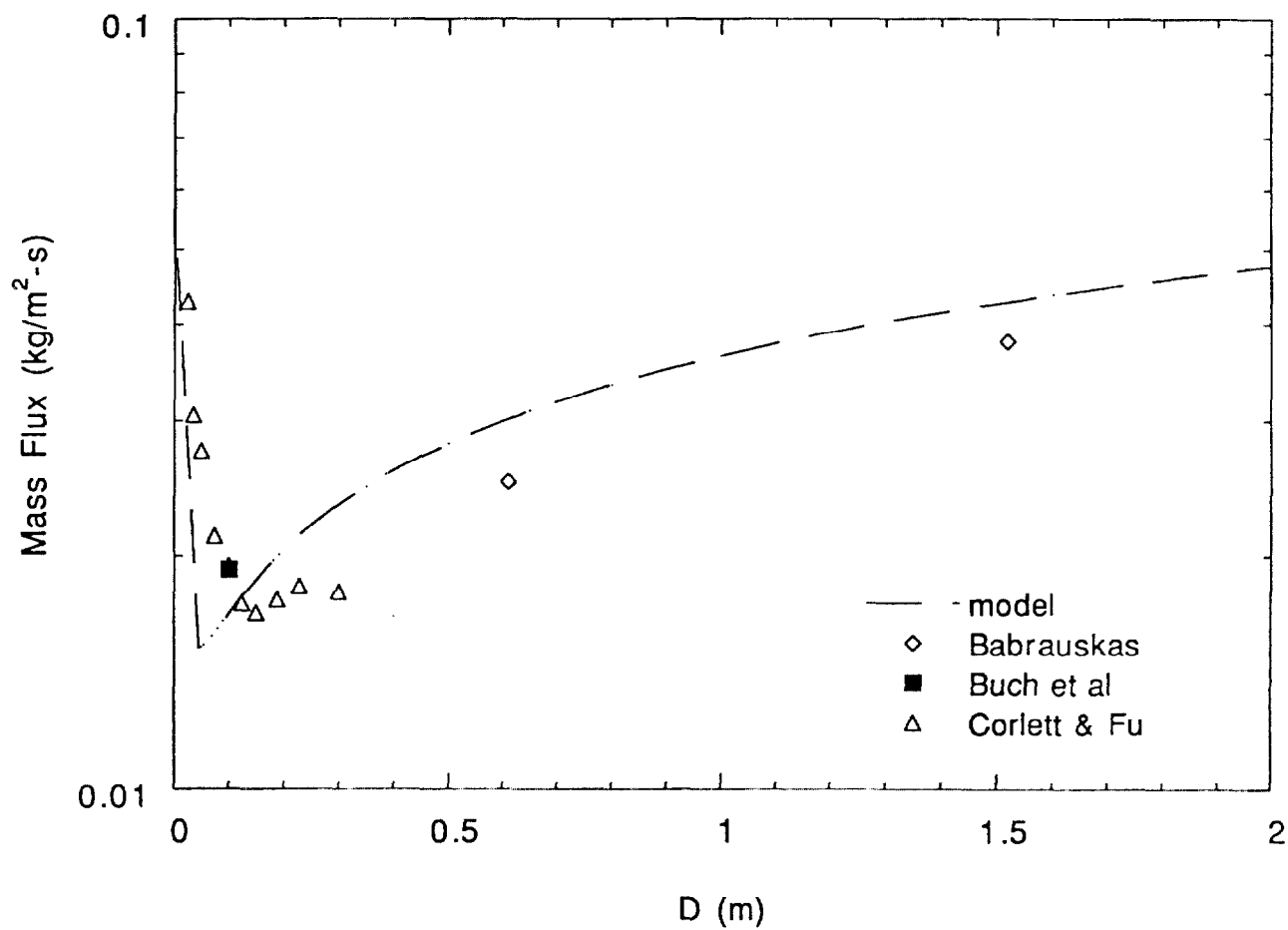


Figure 5. Comparison of experimentally measured mass burning fluxes to those predicted by the model for acetone as a function of pool diameter. Filled symbols represent measurements where the lip height was maintained at a constant value. Open symbols represent measurements where the lip height was varying.

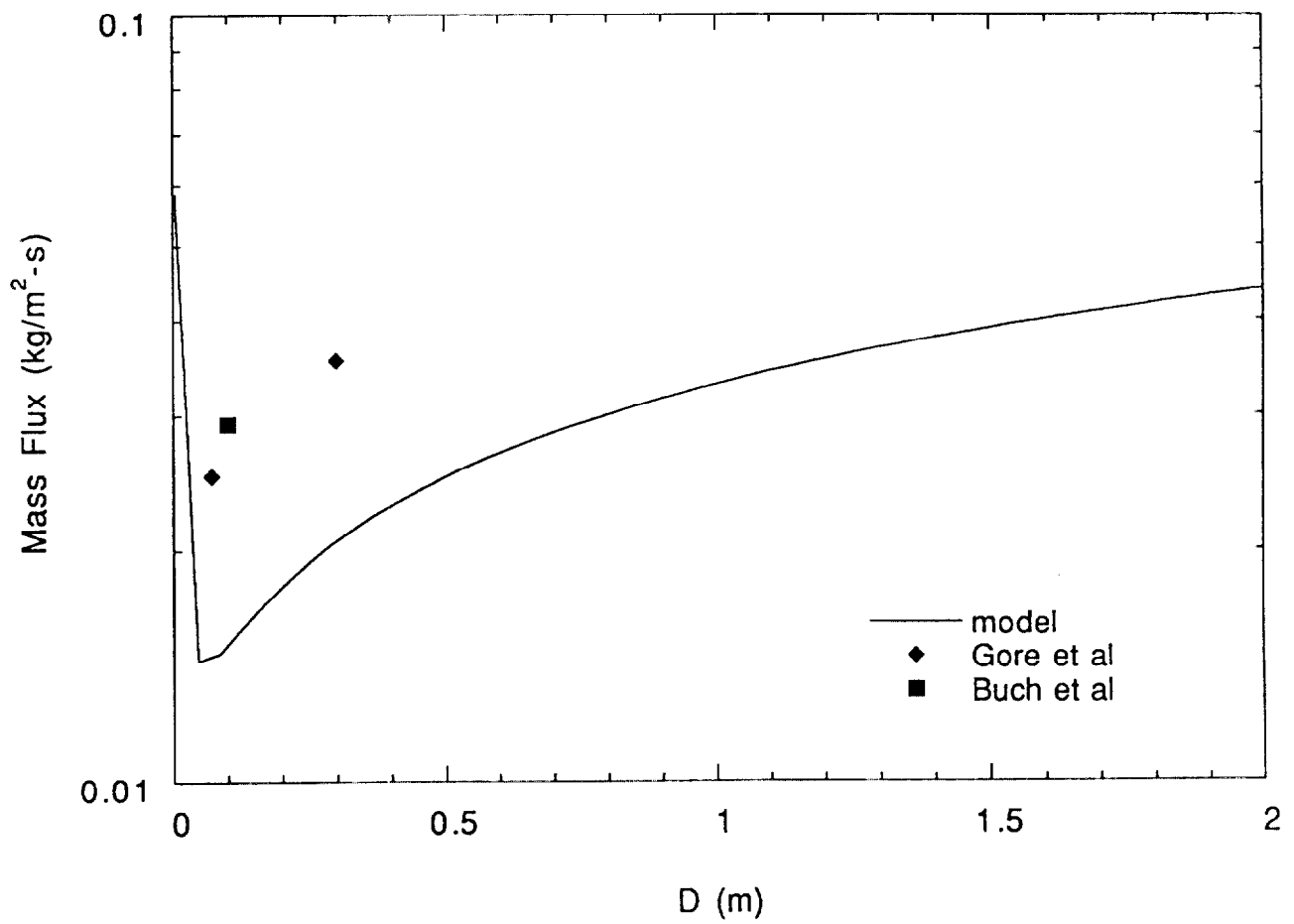


Figure 6. Comparison of experimentally measured mass burning fluxes to those predicted by the model for MMA as a function of pool diameter. Filled symbols represent measurements where the lip height was maintained at a constant value.

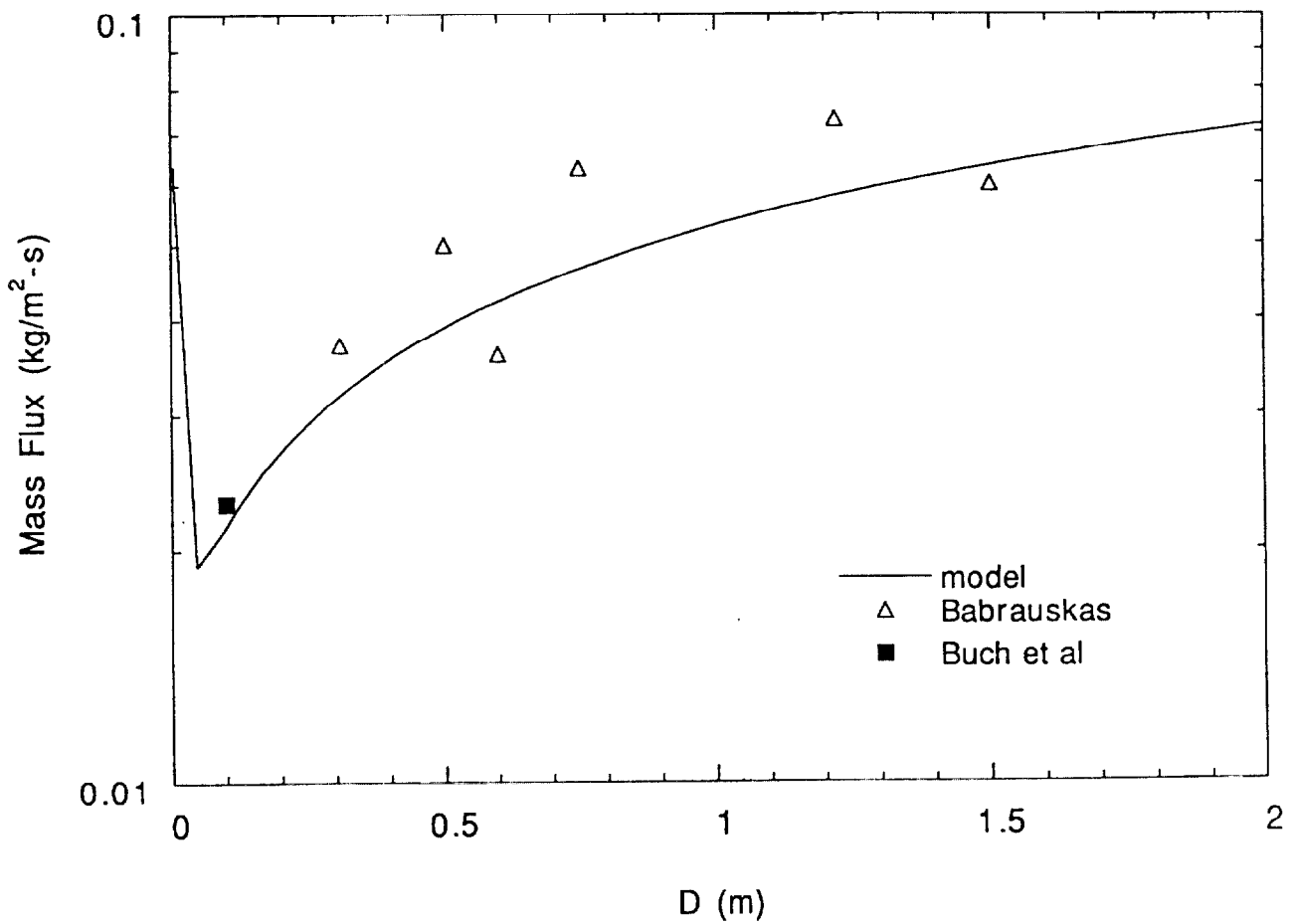


Figure 7. Comparison of experimentally measured burning rates to those predicted by the model for hexane as a function of pool diameter. Filled symbols represent measurements where the lip height was maintained at a constant value. Open symbols represent measurements where the lip height was varying.

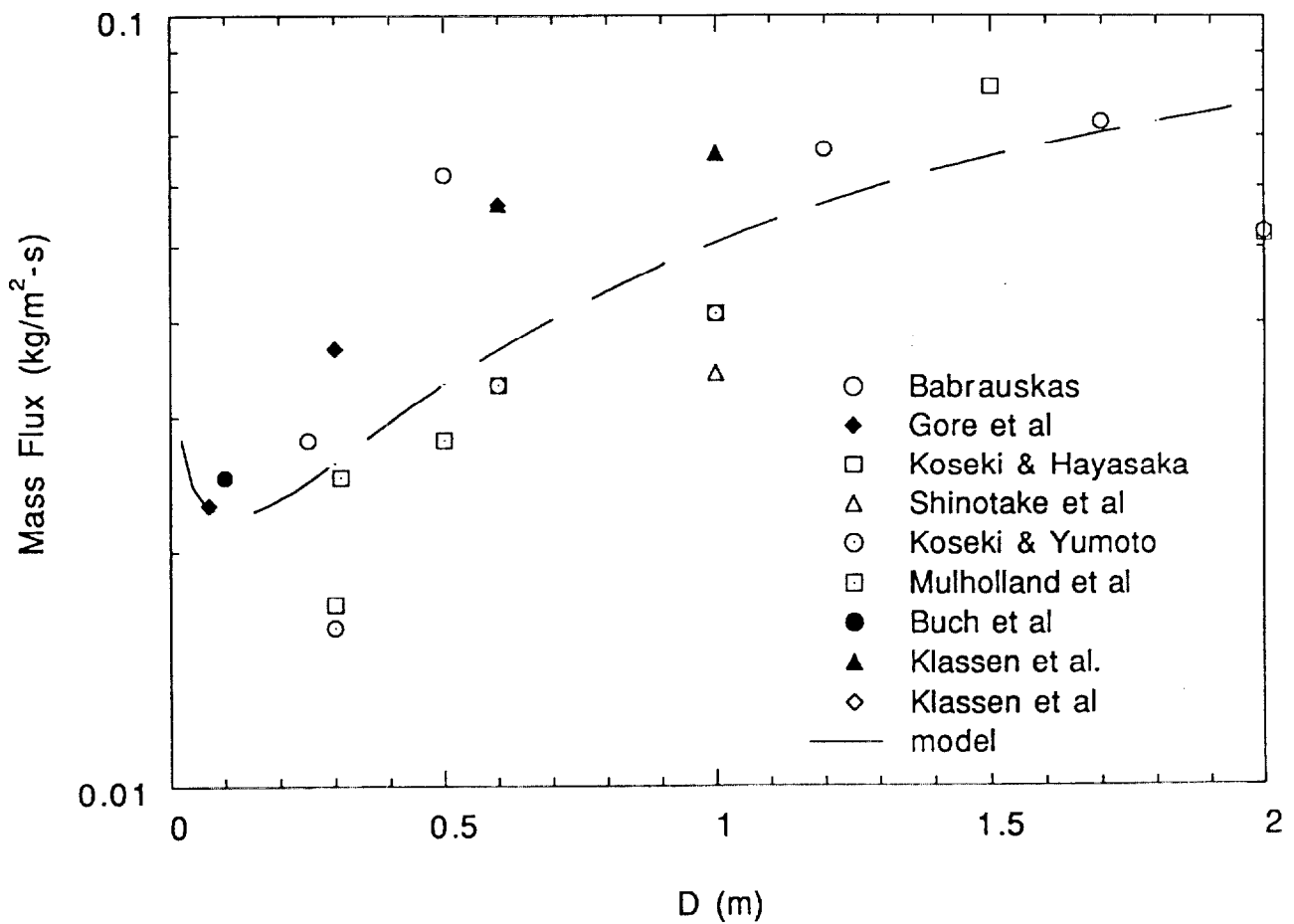


Figure 8. Comparison of experimentally measured burning rates to those predicted by the model for heptane as a function of pool diameter. Filled symbols represent measurements where the lip height was maintained at a constant value. Open symbols represent measurements where the lip height was varying.

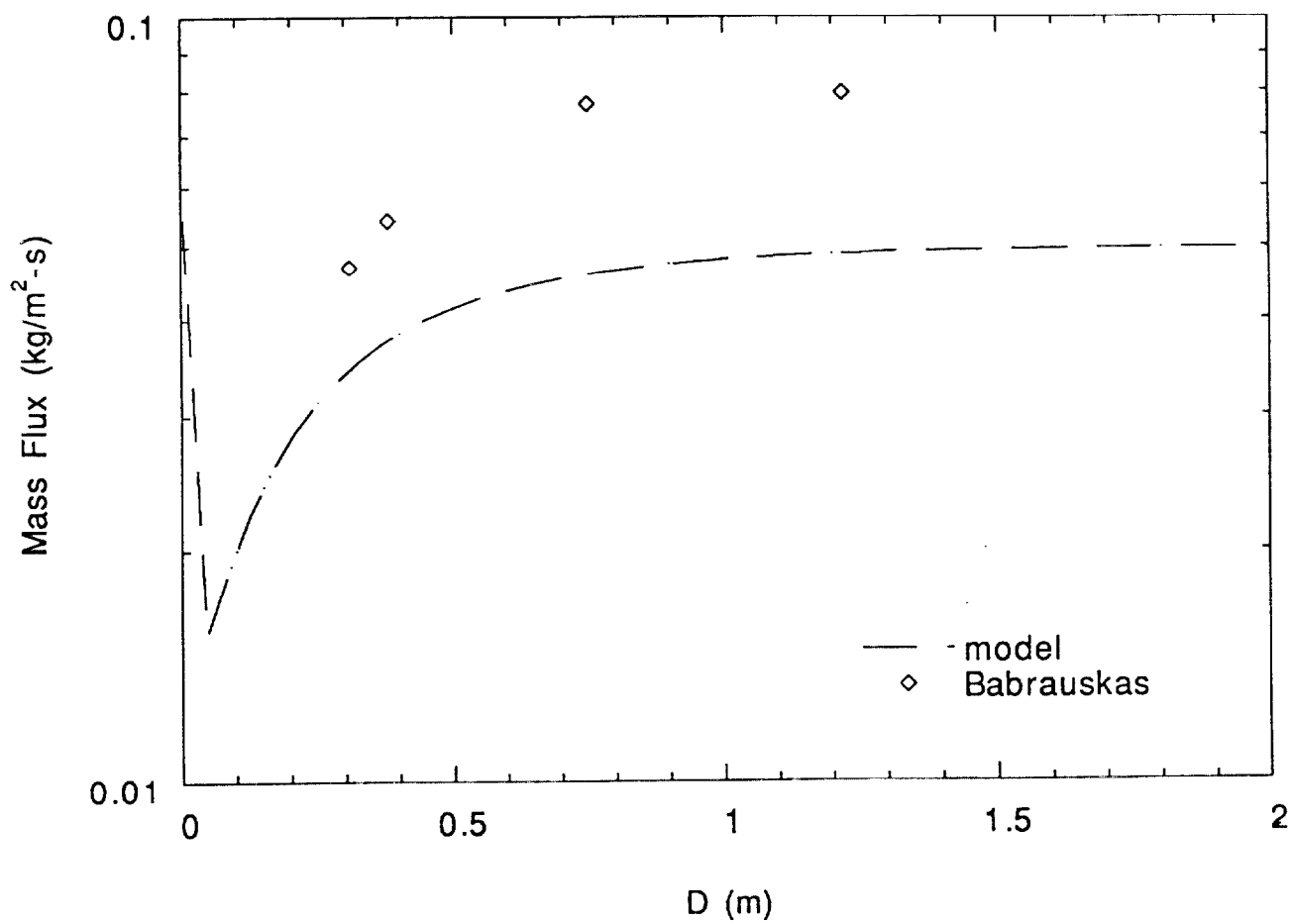


Figure 9. Comparison of experimentally measured mass burning fluxes to those predicted by the model for benzene as a function of pool diameter. Open symbols represent measurements where the lip height was varying.

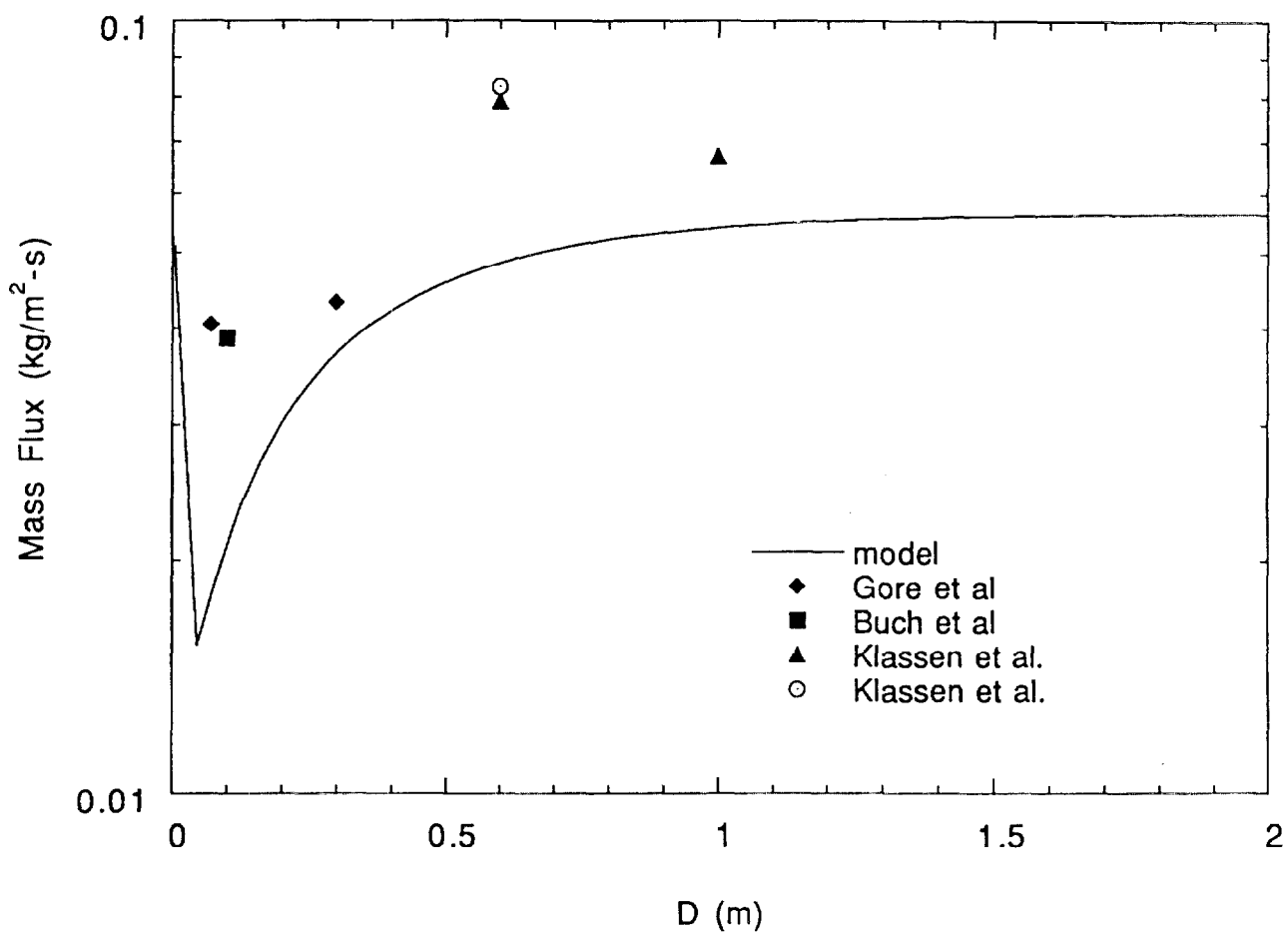


Figure 10. Comparison of experimentally measured mass burning fluxes to those predicted by the model for toluene as a function of pool diameter. Filled symbols represent measurements where the lip height was maintained at a constant value.

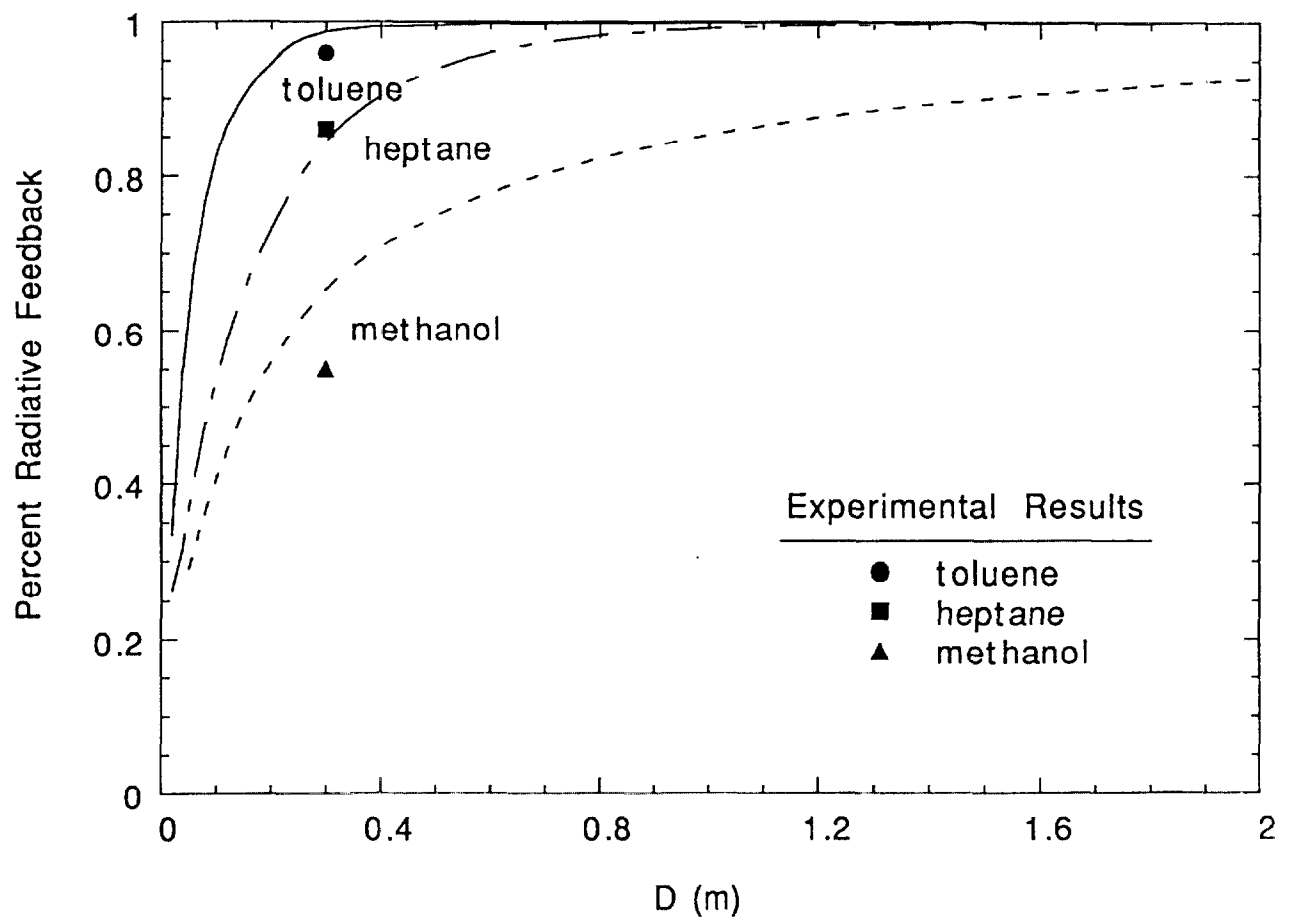


Figure 11 Comparison of the measured [14] and calculated percentage of heat feedback which is radiative as a function of pool diameter for methanol, heptane, and toluene pool fires.

REFERENCES

1. Hottel, H.C., Certain laws governing diffusive burning of liquids. Fire Research Abstract Reviews, **1** (1959) 41-44.
2. Hayasaka, H. & Koseki, H., Estimation of thermal radiation from large pool fires. 11th Joint Meeting of the UJNR Panel on Fire Research and Safety, Berkeley, CA, 1989.
3. Modak, A.T., & Croce, P.C., Plastic pool fires. Combustion and Flame, **30** (1977) 251-265.
4. Orloff, L. & de Ris, J., Froude modeling of pool fires. Factory Mutual Technical Report No. OHON 3.BU RC81-BT-9, Factory Mutual Research, Norwood, MA, 1983.
5. Orloff, L. & de Ris, J., Froude modeling of pool fires. Nineteenth Symp. (Int.) on Combustion, The Combustion Institute, Pittsburgh, PA, 1982, p. 885-895.
6. Burgess, D. & Hertzberg, M., "Radiation from Pool Flames" in Heat Transfer in Flames, N.H. Afgan & J.M. Beers (editors), Scripta Book Co., Washington, D.C., 1974, Chap. 27.
7. Delichatsios, M.A., Air entrainment into buoyant jet flames and pool fires. Combustion and Flame, **70** (1987) 33-46.
8. Smith, J.M. & Van Ness, H.C., Introduction to Chemical Engineering Thermodynamics, 3rd ed., p. 107, 1975, McGraw Hill, NY, NY.
9. Reid, R.C., Prausnitz, J.M., & Sherwood, T.K., The Properties of Gases and Liquids, McGraw-Hill, New York, 3rd ed., 1977.
10. Tewarson, A., Smoke Point Height and Fire Properties of Materials, NIST-GCR-88-555, 1988. National Institute of Standards and Technology, available from National Technical Information Service, Springfield, VA 22161, USA.
11. Gore, J., Klassen, M., Hamins, A., & Kashiwagi, T., Fuel property effects on burning rate and radiative transfer from liquid pool fires. Third Symp. (Int.) on Fire Safety Science, Edinburgh, Scotland, July 1991.
12. American Society of Testing and Materials, E1354-94, Standard test method for heat and visible smoke release rates for materials and products using an oxygen consumption calorimeter, 1994.
13. Siegel, R. & Howell, J.R., Thermal Radiation Heat Transfer, Hemisphere Publishing Corp., 2nd ed., New York, 1981, p. 669.
14. Hamins, A., Klassen, M., Gore, J., Fischer, S., & Kashiwagi, T., Heat feedback to the fuel surface in pool fires, Combustion Science and Technology, **97** (1994) 37-62.

15. Leckner, B., Spectral and total emissivity of water vapor and carbon- dioxide. Combustion and Flame, **19** (1972) 33-48.
16. Yuen, W.W. & Tien, C.L., A simple calculation scheme for the luminous-flame emissivity. Sixteenth Sym. (Int.) on Combustion, The Combustion Institute, Pittsburgh, PA, 1982 p. 1481-1487.
17. Tien, C.L. & Lee, S.C., Flame radiation. Progress in Energy and Combustion Science, **8** (1982) 41-59.
18. Heskestad, G., Structure of turbulent diffusion flames, Fire Safety Journal, **5** (1983) 103-108.
19. Shinotake, A., Koda, S., & Akita, K., An experimental study of radiative properties of pool fires of an intermediate scale. Combustion Science and Technology, **43**, (1985) 85-97.
20. Bard, S. & Pagni, P.J., Carbon particles in small pool fire flames. Journal of Heat Transfer, **103** (1981) 357-362.
21. Gulder, O.L., Influence of hydrocarbon fuel structural constitution and flame temperature on soot formation in laminar diffusion flames. Combustion and Flame, **78** (1989) 179-194.
22. Olson, D.B., Pickens, J.C., & Gill, R.J., The effects of molecular structure on soot formation II. diffusion flames. Combustion and Flame, **62** (1985) 43-60.
23. Yang, J.C., Hamins, A., & Kashiwagi, T., Estimate of the effect of scale on radiative heat loss fraction and combustion efficiency, Combustion Science and Technology, **96** (1994) 183-188.
24. Lockwood, R.W. & Corlett, R.C., Radiative and convective feedback heat flux in small turbulent pool fires with variable pressure and ambient oxygen. Proceedings of the 1987 ASME-JSME Thermal Engineering Joint Conference, Volume 1, p.421-426.
25. Yamamoto, H., Seki, N., & Fukusato, S., Forced convection heat transfer on heated bottom surface of a cavity. Journal of Heat Transfer, **101** (1979) 475-479.
26. Felske, J.D. & Tien, C.L., Calculation of the emissivity of luminous flames. Combustion, Science & Technology, **7** (1973) 25-31.
27. Fischer, S.J., Hardouin-Duparc, B., & Grosshandler, W.L., The structure and radiation of an ethanol pool fire. Combustion and Flame, **70** (1987) 291-306.
28. Koseki, H., & Hayasaka, H., Estimation of thermal balance in heptane pool fire. Journal of Fire Science **7** (1989) 237-249.

29. Koseki, H., & Yumoto, T., Air entrainment and thermal radiation from heptane pool fires, Fire Technology **24** (1988) 33-47.
30. Mulholland, G.W., Henzel, V., & Babrauskas, V., The effect of scale on smoke emission. Second Symposium (International) on Fire Safety Science, editors: T. Wakamatsu et al., Hemisphere Publishing Co., New York, 1989, 347-357.
31. Babrauskas, V., Estimating large pool fire burning rates. Fire Technology, **19** (1983) 251-261.
32. Corlett, R.C., & Fu, T.M., Some recent experiments with pool fires. Pyrodynamics **1** (1966) 253-269.
33. American Society of Testing and Materials, D-1322, Standard test method for smoke points of aviation turbine fuels, 1975, (Re-approved 1980).
34. Buch, R., Hamins, A., Konishi, K., Mattingly, D., & Kashiwagi, T., Radiative emission fraction of pool fires burning silicone fluids. Combustion and Flame, **108** (1997) 118-126.

NIST-114 (REV. 6-93) ADMAN 4.09 U.S. DEPARTMENT OF COMMERCE NATIONAL INSTITUTE OF STANDARDS AND TECHNOLOGY MANUSCRIPT REVIEW AND APPROVAL		(ERB USE ONLY)	
INSTRUCTIONS: ATTACH ORIGINAL OF THIS FORM TO ONE (1) COPY OF MANUSCRIPT AND SEND TO: WEBB SECRETARY, BUILDING 820, ROOM 125		ERB CONTROL NUMBER G	DIVISION
TITLE AND SUBTITLE (CITE IN FULL) A Global Model for Predicting the Burning Rates of Liquid Pool Fires		PUBLICATIONS REPORT NUMBER No. NISTIR 6381	CATEGORY CODE
CONTRACT OR GRANT NUMBER		PUBLICATION DATE	
AUTHOR(S) (LAST NAME, FIRST INITIAL, SECOND INITIAL) Hamins, A., Yang, J.C., & Kashiwagi, T.		NO. PRINTED PAGES	
TYPE OF REPORT AND/OR PERIOD COVERED		PERFORMING ORGANIZATION (CHECK (X) ONE BOX) <input checked="" type="checkbox"/> NIST/GAITHERSBURG <input type="checkbox"/> NIST/BOULDER <input type="checkbox"/> NIST/JILA	
LABORATORY AND DIVISION NAMES (FIRST NIST AUTHOR ONLY) BFRL/864			
SPONSORING ORGANIZATION NAME AND COMPLETE ADDRESS (STREET, CITY, STATE, ZIP)			
PROPOSED FOR NIST PUBLICATION			
<input type="checkbox"/> JOURNAL OF RESEARCH (NIST JRES) <input type="checkbox"/> J. PHYS. & CHEM. REF. DATA (JPCRD) <input type="checkbox"/> HANDBOOK (NIST HB) <input type="checkbox"/> SPECIAL PUBLICATION (NIST SP) <input type="checkbox"/> TECHNICAL NOTE (TN)	<input type="checkbox"/> MONOGRAPH (NIST MN) <input type="checkbox"/> NATL. STD. REF. DATA SERIES (NIST NSRDS) <input type="checkbox"/> FEDERAL INFO. PROCESS. STDS. (NIST FIPS) <input type="checkbox"/> LIST OF PUBLICATIONS (NIST LP) <input checked="" type="checkbox"/> INTERAGENCY/INTERNAL REPORT (NISTIR)	<input type="checkbox"/> LETTER CIRCULAR <input type="checkbox"/> BUILDING SCI. SERIES <input type="checkbox"/> PRODUCT STANDARDS <input type="checkbox"/> OTHER	<input type="checkbox"/> -
PROPOSED FOR NON-NIST PUBLICATION (CITE FULLY): <input type="checkbox"/> -U.S. <input type="checkbox"/> FOREIGN -- <input type="checkbox"/>			
PUBLISHING MEDIUM: <input checked="" type="checkbox"/> PAPER <input type="checkbox"/> DISKETTE <input type="checkbox"/> CD-ROM <input type="checkbox"/> WWW <input type="checkbox"/> OTHER			
SUPPLEMENTARY NOTES			
ABSTRACT (A 2000-CHARACTER OR LESS FACTUAL SUMMARY OF MOST SIGNIFICANT INFORMATION. IF DOCUMENT INCLUDES A SIGNIFICANT BIBLIOGRAPHY OR LITERATURE SURVEY, CITE IT HERE. SPELL OUT ACRONYMS ON FIRST REFERENCE.) (CONTINUE ON SEPARATE PAGE, IF NECESSARY.) A global model is presented which predicts the mass burning flux for pool fires consuming liquid fuels in a quiescent environment. The model assumes constant bulk properties such as flame temperature, soot volume fraction, and species concentration. The computational procedure requires knowledge of the fuel smoke point height and fuel properties such as the heat of vaporization, heat capacity, and boiling point. A cylindrical flame shape is assumed with the flame height given by Heskestad's correlation. A mean beam length approach for radiative heat transfer is utilized and emission from both gas species and soot particles is considered. The convective heat transfer coefficient is estimated using a Raleigh number correlation. Experiments in small diameter pool fire are used to quantify the conductive heat transfer. The predicted mass flux for a number of fuels is within a factor of two of measured burning rates for pool diameters greater than 0.2 m.			
KEY WORDS (MAXIMUM OF 9; 28 CHARACTERS AND SPACES EACH; SEPARATE WITH SEMICOLONS; ALPHABETIC ORDER; CAPITALIZE ONLY PROPER NAMES) burning rate; model studies; pool fires;			
AVAILABILITY: <input checked="" type="checkbox"/> UNLIMITED <input type="checkbox"/> FOR OFFICIAL DISTRIBUTION - DO NOT RELEASE TO NTIS <input type="checkbox"/> ORDER FROM SUPERINTENDENT OF DOCUMENTS, U.S. GPO, WASHINGTON, DC 20402 <input checked="" type="checkbox"/> ORDER FROM NTIS, SPRINGFIELD, VA 22161		NOTE TO AUTHOR(S); IF YOU DO NOT WISH THIS MANUSCRIPT ANNOUNCED BEFORE PUBLICATION, PLEASE CHECK HERE. <input type="checkbox"/>	